

# Summary of research training at CMLA

Marc Kjerland

April 21, 2010

# Contents

<b>1</b>	<b>Single-phase flow</b>	<b>3</b>
1.1	Compressible Euler equations . . . . .	3
1.2	Finite Volume approach . . . . .	4
1.3	Hyperbolicity and the Eigensystem . . . . .	5
1.4	The VFFC Method . . . . .	6
1.5	Handling boundary conditions . . . . .	7
1.5.1	Fluid Conditions . . . . .	8
1.5.2	Wall Conditions . . . . .	10
<b>2</b>	<b>Multi-phase flow</b>	<b>11</b>
2.1	Finite volume integration . . . . .	11
2.2	At the interface . . . . .	12
2.3	Numerical implementation . . . . .	14
2.4	Multiphase boundary conditions . . . . .	16
<b>3</b>	<b>Numerical results</b>	<b>18</b>
3.1	Test case: faucet flow . . . . .	18
3.2	Comparison with incompressible case . . . . .	22

# Introduction

This report is a summary of work done during six months of research training at the Centre de Mathématiques et de Leurs Applications, with funding from l'École Normale Supérieure de Cachan. The subject of this research, directed by Jean-Michel Ghidaglia and Frédéric Dias, is the modeling of two-phase fluid flow, in particular of a slightly-compressible liquid moving through a compressible gas.

The fluids are considered to be inviscid and immiscible, and we use the compressible Euler equations to model the flow. We use the ideal gas law for the thermodynamic equation of state of the gas and we use the stiffened gas law for the equation of state of the liquid.

This work was primarily done using the VFFC-IC method (*Volumes Finis à Flux Caractéristiques with Interface Capture*) [1], in collaboration with Jean-Philippe Braeunig and Daniel Chauveheid. This method uses a direct Eulerian finite volume scheme for the mono-phase flow and a Lagrangian-type scheme at the interface of the fluids. The two-dimensional scheme is presented in this paper, although it has since been scaled to three dimensions.

In Chapter 1, I will focus on the single-phase problem. The methods for multi-phase flow will be detailed in Chapter 2. My contributions to this project are the addition and improvement of fluid boundary conditions for the VFFC-IC method, and the implementation of *ghost* cells for the multiphase case; these contributions will be presented in the appropriate sections. In Chapter 3, I will present some numerical results.

# Chapter 1

## Single-phase flow

### 1.1 Compressible Euler equations

The compressible Euler equations in  $nd$  dimensions can be written in conservation form as:

$$\begin{cases} \partial_t \rho + \nabla \cdot (\rho \mathbf{u}) & = 0, \\ \partial_t (\rho \mathbf{u}) + \nabla \cdot (\rho \mathbf{u} \otimes \mathbf{u} + p \mathbb{I}) & = 0, \\ \partial_t (\rho E) + \nabla \cdot ((\rho E + p) \mathbf{u}) & = 0, \end{cases} \quad (1.1)$$

where  $\rho$  is the density,  $\mathbf{u} \in \mathbb{R}^{nd}$  is the velocity field,  $p$  is pressure, and  $E = e + 0.5 \|\mathbf{u}\|^2$  is the total internal energy with  $e$  being the specific internal energy. A thermodynamic equation of state is necessary to close this system, for which we use the stiffened gas equation:

$$p + \pi = (\gamma - 1) \rho e, \quad (1.2)$$

where  $\gamma$  is the adiabatic index and  $\pi$  is an empirically determined constant for the fluid. Note that for  $\pi = 0$  this is exactly the ideal gas law; for a slightly compressible liquid we use  $\pi \gg 0$ .

It is convenient to write our system of PDEs (1.1) as:

$$\partial_t \mathbf{v} + \nabla \cdot F(\mathbf{v}) = 0, \quad (1.3)$$

where  $\mathbf{v} = \mathbf{v}(\mathbf{x}, t)$  is the vector of conservative variables  $(\rho, \rho \mathbf{u}, \rho E)$ ,  $F$  is a matrix function:

$$\begin{aligned} F : \mathbb{R}^{nd+2} &\longrightarrow \mathbb{R}^{nd+2} \times \mathbb{R}^{nd} \\ \mathbf{v} &\longmapsto F(\mathbf{v}), \end{aligned}$$

and where  $\nabla \cdot F(\mathbf{v}) = \sum_{i=1}^{nd} \partial_{x_i} F^i(\mathbf{v})$ . Of particular importance is the projection

$$F(\mathbf{v}) \cdot \mathbf{n} = (\rho(\mathbf{u} \cdot \mathbf{n}), \rho\mathbf{u}(\mathbf{u} \cdot \mathbf{n}) + p\mathbf{n}, (\rho E + p)(\mathbf{u} \cdot \mathbf{n})). \quad (1.4)$$

## 1.2 Finite Volume approach

The VFFC method (*Volumes Finis à Flux Caractéristiques*), introduced by *Ghidaglia, et al* [1], is a direct Eulerian finite volume scheme. The finite computational domain  $\Omega$  is subdivided into discrete volume elements, and our system advances at discrete time steps  $dt$ . At a given volume element  $K$  we consider an average of the physical variables

$$\mathbf{v}_K(t) = \frac{1}{vol(K)} \int_K \mathbf{v}(\mathbf{x}, t) d\mathbf{x}. \quad (1.5)$$

By integrating (1.3) over  $K$  and applying the divergence theorem, we have

$$vol(K) \frac{d\mathbf{v}}{dt} + \int_{\partial K} F(\mathbf{v}(\sigma, t)) \cdot \mathbf{n}(K, \sigma) d\sigma = 0, \quad (1.6)$$

where  $\mathbf{n}$  is the outward-pointing normal on  $\partial K$ . When the volume elements are polyhedra we have

$$\int_{\partial K} F(\mathbf{v}(\sigma, t)) \cdot \mathbf{n}(K, \sigma) d\sigma = \sum_{L \in N(K)} \mathbf{F}_{K,L}, \quad (1.7)$$

where  $N(K)$  denotes the neighbors of  $K$  and where

$$\mathbf{F}_{K,L} = \int_{K \cap L} F(\mathbf{v}(\sigma, t)) \cdot \mathbf{n}_{KL} d\sigma. \quad (1.8)$$

The crux of the numerical method is finding a suitable approximation to the physical flux terms  $\mathbf{F}_{K,L}$ . This will be the numerical flux  $\phi$  which satisfies

$$\mathbf{F}_{K,L} \approx area(K \cap L) \phi(\mathbf{v}_K, \mathbf{v}_L, \mathbf{n}_{KL}). \quad (1.9)$$

### 1.3 Hyperbolicity and the Eigensystem

We turn our interest to the eigensystem of the Jacobian matrix:

$$J(\mathbf{v}, \mathbf{n}) = \frac{\partial(F(\mathbf{v}) \cdot \mathbf{n})}{\partial \mathbf{v}}. \quad (1.10)$$

The compressible Euler equations form a hyperbolic system of conservation laws; that is, the Jacobian has only real eigenvalues and is diagonalizable. We can determine the eigenvalues  $\lambda_k(\mathbf{v}, \mathbf{n})$ , left eigenvectors  $\mathbf{l}_k(\mathbf{v}, \mathbf{n})$ , and right eigenvectors  $\mathbf{r}_k(\mathbf{v}, \mathbf{n})$ , for  $1 \leq k \leq nd + 2$ , which will satisfy

$$\begin{aligned} {}^t J(\mathbf{v}, \mathbf{n}) \cdot \mathbf{l}_k(\mathbf{v}, \mathbf{n}) &= \lambda_k(\mathbf{v}, \mathbf{n}) \mathbf{l}_k(\mathbf{v}, \mathbf{n}) \\ J(\mathbf{v}, \mathbf{n}) \cdot \mathbf{r}_k(\mathbf{v}, \mathbf{n}) &= \lambda_k(\mathbf{v}, \mathbf{n}) \mathbf{r}_k(\mathbf{v}, \mathbf{n}), \end{aligned} \quad (1.11)$$

with the normalization

$$\mathbf{l}_k(\mathbf{v}, \mathbf{n}) \cdot \mathbf{r}_p(\mathbf{v}, \mathbf{n}) = \delta_{k,p}. \quad (1.12)$$

In the two-dimensional case, where  $\mathbf{u} = (u_x, u_y)$  denotes the velocity,  $\mathbf{n} = (n_x, n_y)$  the unit normal, and for some  $\mathbf{t} = (t_x, t_y)$  such that  $\mathbf{t} \cdot \mathbf{n} = 0$ , we have:

$$\begin{aligned} \lambda_1(\mathbf{v}, \mathbf{n}) &= \mathbf{u} \cdot \mathbf{n} - c, \\ \lambda_2(\mathbf{v}, \mathbf{n}) &= \mathbf{u} \cdot \mathbf{n}, \\ \lambda_3(\mathbf{v}, \mathbf{n}) &= \mathbf{u} \cdot \mathbf{n}, \\ \lambda_4(\mathbf{v}, \mathbf{n}) &= \mathbf{u} \cdot \mathbf{n} + c, \end{aligned} \quad (1.13)$$

$$\mathbf{R}(\mathbf{v}, \mathbf{n}) = \begin{pmatrix} 1 & 1 & 0 & 1 \\ u_x - cn_x & u_x & t_x & u_x + cn_x \\ u_y - cn_y & u_y & t_y & u_y + cn_y \\ H - c(\mathbf{n} \cdot \mathbf{u}) & H - \frac{c^2}{k} & (\mathbf{t} \cdot \mathbf{u}) & H + c(\mathbf{n} \cdot \mathbf{u}) \end{pmatrix}, \quad (1.14)$$

$$\mathbf{L}(\mathbf{v}, \mathbf{n}) = \frac{1}{2c^2} \begin{pmatrix} K + c(\mathbf{n} \cdot \mathbf{u}) & 2k(H - \|\mathbf{u}\|^2) & -2c^2(\mathbf{t} \cdot \mathbf{u}) & K - c(\mathbf{n} \cdot \mathbf{u}) \\ -ku_x - cn_x & 2ku_x & 2c^2 t_x & -ku_x + cn_x \\ -ku_y - cn_y & 2ku_y & 2c^2 t_y & -ku_y + cn_y \\ k & -2k & 0 & k \end{pmatrix}, \quad (1.15)$$

where

$$\begin{aligned}
c &= \sqrt{\frac{\gamma p + \pi}{\rho}} \quad (\text{speed of sound}), \\
H &= e + \frac{p}{\rho} + \frac{1}{2} \|\mathbf{u}\|^2 \quad (\text{total enstrophy}), \\
k &= \frac{1}{\rho} \left( \frac{\partial p}{\partial e} \right), \\
\text{and } K &= c^2 + k(\|\mathbf{u}\|^2 - H).
\end{aligned} \tag{1.16}$$

## 1.4 The VFFC Method

In order to approximate the physical flux on a face  $\Gamma$  between two volume elements  $K$  and  $L$ , we take  $\mathbf{v}_\Gamma$  to be an average of the conserved variables of the bordering cells, such as:

$$\mathbf{v}_\Gamma = \frac{\text{vol}_K \mathbf{v}_L + \text{vol}_L \mathbf{v}_K}{\text{vol}_K + \text{vol}_L}. \tag{1.17}$$

By multiplying (1.3) by the Jacobian matrix and considering only evolution in the normal direction  $\mathbf{n}$  from  $K$  to  $L$ , we arrive at the following equation:

$$\partial_t (F(\mathbf{v}_\Gamma) \cdot \mathbf{n}) + J(\mathbf{v}_\Gamma, \mathbf{n}) \partial_n (F(\mathbf{v}_\Gamma) \cdot \mathbf{n}) = 0, \tag{1.18}$$

where  $\partial_n = \mathbf{n} \cdot \nabla$ . Thus we have Riemann invariants which travel in the direction of  $\mathbf{n}$  with speed  $\lambda_k(\mathbf{v}_\Gamma, \mathbf{n})$ :

$$(\partial_t + \lambda_k(\mathbf{v}_\Gamma, \mathbf{n}) \partial_n) (\mathbf{l}_k(\mathbf{v}_\Gamma, \mathbf{n}) \cdot F(\mathbf{v}_\Gamma) \cdot \mathbf{n}) = 0. \tag{1.19}$$

We solve this equation in one dimension using the method of characteristics and an *upwind* discretization:

- If  $\lambda_k(\mathbf{v}_\Gamma, \mathbf{n}) > 0$ , then  $\mathbf{l}_k(\mathbf{v}_\Gamma, \mathbf{n}) \cdot \phi(\mathbf{v}_K, \mathbf{v}_L, \mathbf{n}) = \mathbf{l}_k(\mathbf{v}_\Gamma, \mathbf{n}) \cdot (F(\mathbf{v}_K) \cdot \mathbf{n})$ .
- If  $\lambda_k(\mathbf{v}_\Gamma, \mathbf{n}) < 0$ , then  $\mathbf{l}_k(\mathbf{v}_\Gamma, \mathbf{n}) \cdot \phi(\mathbf{v}_K, \mathbf{v}_L, \mathbf{n}) = \mathbf{l}_k(\mathbf{v}_\Gamma, \mathbf{n}) \cdot (F(\mathbf{v}_L) \cdot \mathbf{n})$ .
- If  $\lambda_k(\mathbf{v}_\Gamma, \mathbf{n}) = 0$ , then  $\mathbf{l}_k(\mathbf{v}_\Gamma, \mathbf{n}) \cdot \phi(\mathbf{v}_K, \mathbf{v}_L, \mathbf{n}) = \mathbf{l}_k(\mathbf{v}_\Gamma, \mathbf{n}) \cdot \left( \frac{F(\mathbf{v}_K) + F(\mathbf{v}_L)}{2} \cdot \mathbf{n} \right)$ .

We can thus write the flux term explicitly as

$$\phi(\mathbf{v}_K, \mathbf{v}_L, \mathbf{n}) = \left( \frac{F(\mathbf{v}_K) + F(\mathbf{v}_L)}{2} - \text{sign}(J(\mathbf{v}_\Gamma, \mathbf{n})) \frac{F(\mathbf{v}_K) - F(\mathbf{v}_L)}{2} \right) \cdot \mathbf{n}, \quad (1.20)$$

where

$$\text{sign}(J(\mathbf{v}_\Gamma, \mathbf{n})) = R(\mathbf{v}_\Gamma, \mathbf{n}) \text{diag}(\text{sign}(\lambda(\mathbf{v}_\Gamma, \mathbf{n}))) L(\mathbf{v}_\Gamma, \mathbf{n}).$$

Note that the numerical flux is both consistent and conservative:

$$\phi(\mathbf{v}_K, \mathbf{v}_K, \mathbf{n}) = F(\mathbf{v}_K) \cdot \mathbf{n} \quad (1.21)$$

$$\phi(\mathbf{v}_K, \mathbf{v}_L, \mathbf{n}) = -\phi(\mathbf{v}_L, \mathbf{v}_K, \mathbf{n}) \quad (1.22)$$

Finally, the time step  $dt$  is determined by a Courant-Friedrichs-Levy (CFL) stability condition:

$$dt < \min_i \left( \frac{vol_i}{A \max_k |(\lambda_i)|} \right) \quad (1.23)$$

## 1.5 Handling boundary conditions

Common boundary conditions used with this method are periodic, wall, and fluid conditions. Here we will address the latter two conditions. Let  $\phi(\mathbf{v}_K, K, \mathbf{n})$  denote the numerical flux for a volume element  $K$  at the boundary with outward normal  $\mathbf{n}$ .

In general this problem will be ill-posed if we impose either  $\mathbf{v}$  or  $F(\mathbf{v}) \cdot \mathbf{n}$  as boundary conditions. This can be understood by analyzing the linearized problem:

$$\partial_t \mathbf{v} + J(\mathbf{v}, \mathbf{n}) \partial_n \mathbf{v} = 0. \quad (1.24)$$

For a positive eigenvalue  $\lambda_k(\mathbf{v}, \mathbf{n}) > 0$ , by the method of characteristics we have scalar information propagated in the direction of  $\mathbf{n}$ , and in the opposite direction for a negative eigenvalue. For the nonlinear problem, recall that for  $\lambda_k(\mathbf{v}_K, \mathbf{n}) > 0$  we have

$$\mathbf{l}_k(\mathbf{v}_K, \mathbf{n}) \cdot \phi(\mathbf{v}_K, K, \mathbf{n}) = \mathbf{l}_k(\mathbf{v}_K, \mathbf{n}) \cdot (F(\mathbf{v}_K) \cdot \mathbf{n}). \quad (1.25)$$



Thus for each positive eigenvalue we have scalar information at the boundary which is propagated from the interior of  $\Omega$ . Similarly, for each negative eigenvalue  $\lambda_k(\mathbf{v}_K, \mathbf{n}) < 0$  we need external scalar information. For a more detailed treatment, see *Ghidaglia & Pascal*, [2].

### 1.5.1 Fluid Conditions

Here we address fluid boundary conditions, where there is nonzero normal velocity at the boundary  $\partial\Omega$ . The eigenvalues (1.13) are functions of  $\mathbf{u} \cdot \mathbf{n}$ , so we will look at several cases individually.

#### Supersonic outlet: $\mathbf{u} \cdot \mathbf{n} > c$

Here all the eigenvalues are positive, so all the information at the boundary is determined by the interior physical state. Thus

$$\phi(\mathbf{v}_K, K, \mathbf{n}) = F(\mathbf{v}_K) \cdot \mathbf{n}. \quad (1.26)$$

#### Supersonic inlet: $\mathbf{u} \cdot \mathbf{n} < -c$

Here all the eigenvalues are negative, so all the information at the boundary is determined externally. The flux is determined solely from given physical conditions outside the domain:

$$\phi(\mathbf{v}_K, K, \mathbf{n}) = F(\mathbf{v}_{\text{given}}) \cdot \mathbf{n}. \quad (1.27)$$

It should be noted that flows with large Mach numbers are very difficult to resolve numerically in this framework, so these supersonic conditions are in practice not yet resolvable.

#### Subsonic outlet: $0 < \mathbf{u} \cdot \mathbf{n} < c$

Here only one eigenvalue is negative and the rest are positive. Let  $\phi(\mathbf{v}_K, K, \mathbf{n}) = F(\mathbf{v}) \cdot \mathbf{n}$ . Then we need to prescribe one physical boundary condition, and from (1.25) we have:

$$\begin{aligned} \mathbf{l}_k(\mathbf{v}_K, \mathbf{n}) \cdot (F(\mathbf{v}) \cdot \mathbf{n}) &= l_k(\mathbf{v}_K, \mathbf{n}) \cdot (F(\mathbf{v}_K) \cdot \mathbf{n}), \\ \text{for } k &= 2, \dots, nd + 2. \end{aligned} \quad (1.28)$$

Then from the normalization (1.12) we have:

$$\begin{aligned}
F(\mathbf{v}) \cdot \mathbf{n} &= \sum_{k=1}^{nd+2} (l_k(\mathbf{v}_K, \mathbf{n}) \cdot (F(\mathbf{v}) \cdot \mathbf{n})) \mathbf{r}_k(\mathbf{v}_K, \mathbf{n}) \\
&= F(\mathbf{v}_K) \cdot \mathbf{n} + (\mathbf{l}_1(\mathbf{v}_K, \mathbf{n}) \cdot (F(\mathbf{v}) \cdot \mathbf{n} - F(\mathbf{v}_K) \cdot \mathbf{n})) \mathbf{r}_1(\mathbf{v}_K, \mathbf{n}).
\end{aligned} \tag{1.29}$$

So  $F(\mathbf{v}) \cdot \mathbf{n}$  is just a slight perturbation from  $F(\mathbf{v}_K) \cdot \mathbf{n}$ . If, for example, we were to prescribe a physical boundary condition  $p = p_{given}$ , then to determine  $\phi(\mathbf{v}_K, K, \mathbf{n})$  we simply need to solve the system:

$$\begin{cases} F(\mathbf{v}) \cdot \mathbf{n} = F(\mathbf{v}_K) \cdot \mathbf{n} + \epsilon \mathbf{r}_1(\mathbf{v}_K, \mathbf{n}) \\ \epsilon \in \mathbb{R} \text{ such that } p = p_{given}, \end{cases} \tag{1.30}$$

which can be solved using the Newton-Raphson method.

**Subsonic inlet:**  $-c < \mathbf{u} \cdot \mathbf{n} < 0$

Here only  $\lambda_{nd+2}(\mathbf{v}_K, \mathbf{n}) > 0$  and the remaining eigenvalues are negative. Thus we impose  $nd + 1$  conditions, and the remaining condition must be calculated to satisfy:

$$\mathbf{l}_{nd+2}(\mathbf{v}_K, \mathbf{n}) \cdot (F(\mathbf{v}) \cdot \mathbf{n}) = \mathbf{l}_{nd+2}(\mathbf{v}_K, \mathbf{n}) \cdot (F(\mathbf{v}_K) \cdot \mathbf{n}). \tag{1.31}$$

We have many possible options for prescribing physical boundary conditions in this case. One possibility might be to impose  $\rho = \rho_{given}, p = p_{given}$ , and  $\mathbf{u} = \mu \hat{\mathbf{u}}_{given}$ , for some magnitude  $\mu$  to be determined. In another scenario, one could prescribe  $(\rho, \mathbf{u})$  and solve for  $p$ . Since we know  $\mathbf{l}_{nd+2}$  and  $F(\mathbf{v}_K) \cdot \mathbf{n}$ , we simply expand (1.31) and solve for the single unknown. Using the notation  $\mathbf{l}_{nd+2} = (\underline{L}^1, \underline{\mathbf{L}}, \underline{L}^{nd+2})$ , we have the following equation:

$$\begin{aligned}
\rho(\hat{\mathbf{u}} \cdot \mathbf{n}) \left( \frac{1}{2} \mu^3 \underline{L}^1 + \mu^2 (\hat{\mathbf{u}} \cdot \underline{\mathbf{L}}) + \mu ((\underline{L}^1 + h \underline{L}^{nd+2}) + p(\underline{\mathbf{L}} \cdot \mathbf{n})) \right) \\
= \mathbf{l}_{nd+2} \cdot (F(\mathbf{v}_K) \cdot \mathbf{n})
\end{aligned} \tag{1.32}$$

### 1.5.2 Wall Conditions

At a wall with outward normal  $\mathbf{n}$ , we have the condition  $\mathbf{u} \cdot \mathbf{n} = 0$ . Thus the normal flux is given by

$$F(\mathbf{v}) \cdot \mathbf{n} = (0, p\mathbf{n}, 0). \quad (1.33)$$

To determine this flux, we simply find the unknown  $p$  by solving (1.31):

$$p = \frac{\mathbf{l}_{nd+2}(\mathbf{v}_K, \mathbf{n}) \cdot (F(\mathbf{v}_K) \cdot \mathbf{n})}{\mathbf{l}_{nd+2}(\mathbf{v}_K, \mathbf{n}) \cdot (0, \mathbf{n}, 0)}. \quad (1.34)$$

## Chapter 2

# Multi-phase flow

We now consider the multi-phase flow problem. Here the domain contains two different fluids, such as air and water, assumed to be immiscible and inviscid at the interface. Each fluid flow obeys the compressible Euler equations, differing only in the parameters  $\pi$  and  $\gamma$  in their respective equations of state.

### 2.1 Finite volume integration

In general the interface between two fluids will be non-stationary. Thus in the multi-phase problem we must consider fluid volumes whose boundaries are variable in time. Suppose we have such a domain  $\Omega(t)$  whose boundary has nonzero velocity:

$$\partial\Omega(t) = \Gamma(t) = \Gamma_{u \cdot n = 0} \cup \Gamma_{u \cdot n \neq 0}. \quad (2.1)$$

We use the following result:

$$\frac{d}{dt} \int_{\Omega(t)} \mathbf{v} dS = \int_{\Omega(t)} \frac{\partial \mathbf{v}}{\partial t} dS + \int_{\partial\Omega(t)} \mathbf{v} (\mathbf{u}_{int} \cdot \mathbf{n}_{int}) d\sigma, \quad (2.2)$$

where  $\mathbf{u}_{int}$  denotes the velocity of the interface  $\partial\Omega(t)$ . By integrating the system over  $\Omega$  we have:

$$\begin{aligned} 0 &= \int_{\Omega(t)} (\partial_t \mathbf{v} + \nabla \cdot F(\mathbf{v})) dS = \\ &= \frac{d}{dt} \int_{\Omega(t)} \mathbf{v} dS - \int_{\partial\Omega(t)} \mathbf{v} (\mathbf{u}_{int} \cdot \mathbf{n}_{int}) d\sigma + \int_{\partial\Omega(t)} F(\mathbf{v}) \cdot \mathbf{n} d\sigma. \end{aligned} \quad (2.3)$$

Noting that  $F(\mathbf{v}) = \mathbf{v}(\mathbf{u} \cdot \mathbf{n}) + p\mathbf{N}$ , where  $\mathbf{N} = (0, \mathbf{n}, \mathbf{u} \cdot \mathbf{n})^t$ , we have:

$$= \frac{d}{dt} \int_{\Omega(t)} \mathbf{v} dS + \int_{\Gamma_{u \cdot n \neq 0}} p_{int} \mathbf{N}_{int} d\sigma + \int_{\Gamma_{u \cdot n = 0}} F(\mathbf{v}) \cdot \mathbf{n} d\sigma. \quad (2.4)$$

So we arrive at the following finite volume scheme:

$$\frac{|\Omega^{n+1}| \mathbf{v}^{n+1} - |\Omega^n| \mathbf{v}^n}{\Delta t} + \sum_{\Gamma_{u \cdot n = 0}} area(\Gamma) \phi_\Gamma + \sum_{\Gamma_{u \cdot n \neq 0}} area(\Gamma) p_{int} \mathbf{N}_{int} = 0. \quad (2.5)$$

## 2.2 At the interface

To understand the dynamics at the interface of the two fluids, it is convenient to consider the problem in Lagrangian coordinates. The compressible Euler equations in a 1D Lagrangian formulation are given by:

$$\partial_t \begin{pmatrix} \tau \\ u \\ E \end{pmatrix} + \partial_x \begin{pmatrix} -u \\ p \\ pu \end{pmatrix} = 0, \quad (2.6)$$

where  $\tau = \frac{1}{\rho}$ . The fundamental thermodynamics equation  $Tds = de + pd\tau$  yields

$$\begin{aligned} T\partial_t s &= \partial_t e + p\partial_t \tau \\ &= -\partial_t \left( \frac{1}{2} u^2 \right) - \partial_x (pu) + p\partial_x u \\ &= -u\partial_t u - u\partial_x p \\ &= 0. \end{aligned} \quad (2.7)$$

The change of variables  $\varphi : (\tau, u, s) \rightarrow (\tau, u, E)$  transforms (2.6) into:

$$\begin{cases} \partial_t \tau - \partial_x u = 0 \\ \partial_t u + \partial_x p = 0 \\ \partial_t s = 0 \end{cases} \quad (2.8)$$

The Jacobian matrix for this system is given by

$$A(\mathbf{V}) = \begin{pmatrix} 0 & -1 & 0 \\ -\rho^2 c^2 & 0 & p_s \\ 0 & 0 & 0 \end{pmatrix}, \quad (2.9)$$

with eigenvalues

$$\lambda_{-1} = -\rho c < \lambda_0 = 0 < \lambda_1 = \rho c, \quad (2.10)$$

right eigenvectors

$$\mathbf{r}_{-1} = \begin{pmatrix} \rho^{-1} \\ c \\ 0 \end{pmatrix}, \mathbf{r}_0 = \begin{pmatrix} p_s \\ 0 \\ \rho^2 c^2 \end{pmatrix}, \mathbf{r}_1 = \begin{pmatrix} \rho^{-1} \\ -c \\ 0 \end{pmatrix}, \quad (2.11)$$

and left eigenvectors

$$\mathbf{l}_{-1} = \begin{pmatrix} \rho c \\ 1 \\ p_s (\rho c)^{-1} \end{pmatrix}, \mathbf{l}_0 = \begin{pmatrix} 0 \\ 0 \\ (\rho c)^{-2} \end{pmatrix}, \mathbf{l}_1 = \begin{pmatrix} \rho c \\ -1 \\ p_s (\rho c)^{-1} \end{pmatrix}. \quad (2.12)$$

It is easy to verify that the flux term satisfies the equation

$$\partial_t F(\mathbf{V}) + A(\mathbf{V}) \partial_x F(\mathbf{V}) = 0 \quad (2.13)$$

Consider an interface which separates two states  $\mathbf{V}^-$  and  $\mathbf{V}^+$ . Linearizing yields

$$\begin{aligned} (E^-) : \quad & \partial_t \mathbf{F}(\mathbf{V}) + A(\mathbf{V}^-) \partial_x \mathbf{F}(\mathbf{V}) = 0 \\ (E^+) : \quad & \partial_t \mathbf{F}(\mathbf{V}) + A(\mathbf{V}^+) \partial_x \mathbf{F}(\mathbf{V}) = 0. \end{aligned} \quad (2.14)$$

For  $(E^-)$ , the Riemann invariant associated with the eigenvalue  $\rho^- c^-$  is given by

$$\pi^- = \mathbf{l}_1^- \cdot \mathbf{F}(\mathbf{V}) = \begin{pmatrix} \rho^- c^- \\ -1 \\ p_s (\rho^- c^-)^{-1} \end{pmatrix} \cdot \begin{pmatrix} -u \\ p \\ 0 \end{pmatrix} = -p - \rho^- c^- u; \quad (2.15)$$

For  $(E^+)$ , the Riemann invariant associated with the eigenvalue  $-\rho^+c^+$  is given by

$$\pi^+ = \mathbf{l}_{-1}^+ \cdot \mathbf{F}(\mathbf{V}) = \begin{pmatrix} \rho^+c^+ \\ 1 \\ p_s(\rho^+c^+)^{-1} \end{pmatrix} \cdot \begin{pmatrix} -u \\ p \\ 0 \end{pmatrix} = p - \rho^+c^+u. \quad (2.16)$$

Using an upwind discretization method one can write

$$\pi^-(\mathbf{V}^-) = \pi^-(\mathbf{V}_{int}) \quad \text{and} \quad \pi^+(\mathbf{V}^+) = \pi^+(\mathbf{V}_{int}), \quad (2.17)$$

which leads to the relation

$$\begin{cases} p_{int} = \frac{\rho^+c^+p^- + \rho^-c^-p^+}{\rho^-c^- + \rho^+c^+} + \rho^-c^-\rho^+c^+ \frac{u^- - u^+}{\rho^-c^- + \rho^+c^+} \\ u_{int} = \frac{\rho^+c^+p^+ + \rho^-c^-p^-}{\rho^-c^- + \rho^+c^+} + \frac{p^- + p^+}{\rho^-c^- + \rho^+c^+} \end{cases} \quad (2.18)$$

first derived by Braeunig (2007).

### 2.3 Numerical implementation

When we discretize the spatial domain  $\Omega$ , we assign a volume fraction  $\alpha \in [0, 1]$  and a normal vector to each volume element. A volume element with  $\alpha = 0$  contains only air, a volume element with  $\alpha = 1$  contains only water, and other values of  $\alpha$  in mixed cells correspond to intermediate fractional mixtures. In volume elements with  $\alpha \in (0, 1)$  the normal vector represents the normal direction to the interface. From these two values we can reconstruct a linear approximation to the interface in each cell.

The VFFC scheme uses a regular rectangular mesh, for which we use a two-step directional splitting. At each time step we traverse the grid in 1D, and for cells around the interface we use the method of *condensates* developed by Braeunig (2007) [4]. In this method, we consider a group of cells near an interface, calculate the evolution of the interface in a Lagrangian framework, and project this back onto the Eulerian grid, as shown in the following schematic:

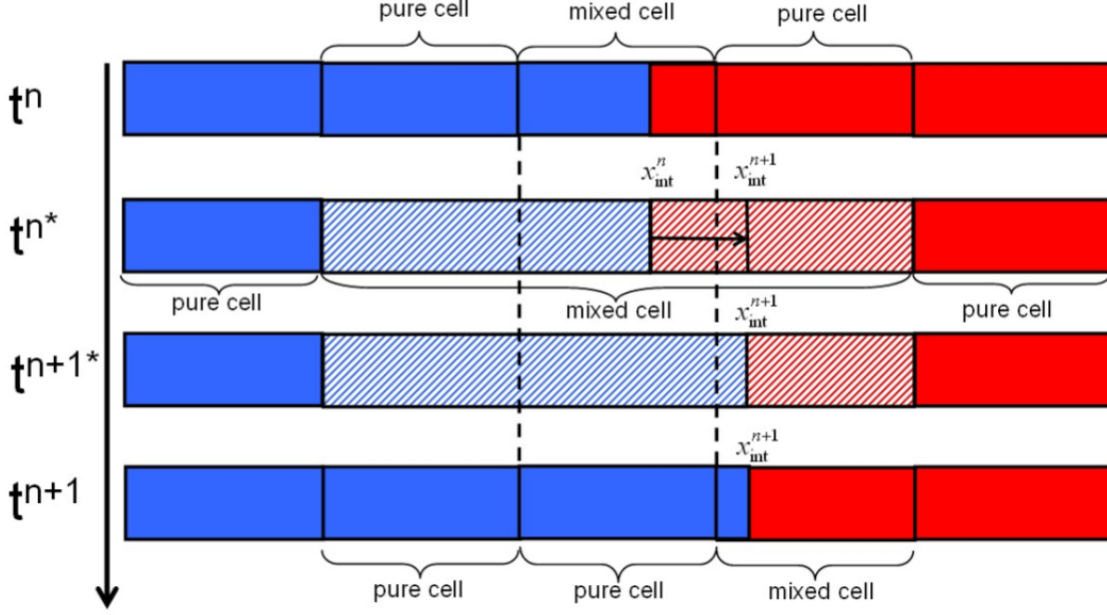


Figure 2.1: Using the condensate for mixed cells

The condensate is a 1D structure consisting of  $nc$  layers of different materials, separated by  $nc - 1$  interfaces. Each layer is associated with layer-centered conservative variables and each interface is associated with a normal vector. The boundaries of a condensate are stationary edges for which we compute Eulerian flux terms. For example, in Figure 2.1, where  $nc = 2$ , the conservative variables are calculated as:

$$\begin{aligned}\tilde{V}_1 &= \frac{Vol_1 V_1 + Vol_{pure1} V_{pure1}}{Vol_1 + Vol_{pure1}} \\ \tilde{V}_2 &= \frac{Vol_2 V_2 + Vol_{pure2} V_{pure2}}{Vol_2 + Vol_{pure2}}.\end{aligned}\tag{2.19}$$

We calculate the evolution of the condensate based on (2.5) and (2.18). For internal volume elements, the condensate is formed from adjacent mixed cells and two bordering pure cells, and the CFL condition (1.23) ensures that the interface will not move outside the condensate in a single time step. Following the directional splitting, the normal vectors for the interface are recalculated using a method by *Youngs* [3] based on an approximation to the gradient of the volume fraction in a mixed



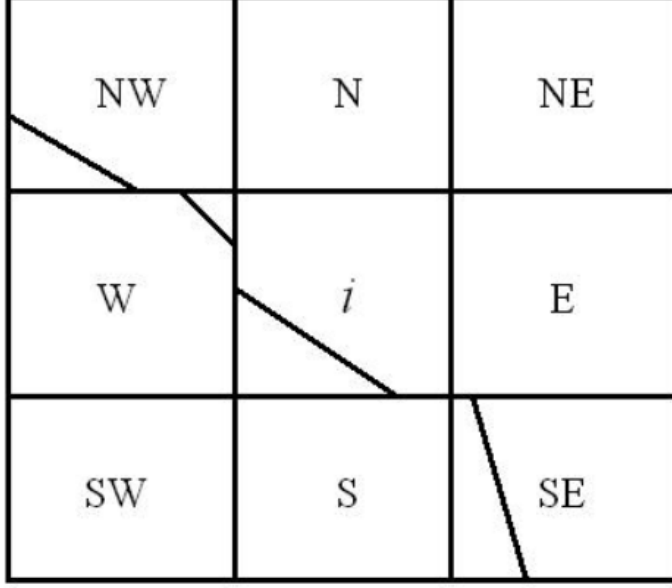


Figure 2.2: Reconstruction of the interface in 2D

cell  $i$ :

$$\mathbf{n}_i = -\frac{\nabla\alpha_i}{\|\nabla\alpha_i\|}, \quad (2.20)$$

where

$$\begin{aligned} \frac{\partial\alpha_i}{\partial x} &= \frac{(\alpha_{NE} + 2\alpha_E + \alpha_{SE}) - (\alpha_{NW} + 2\alpha_W + \alpha_{SW})}{8\Delta x} \\ \frac{\partial\alpha_i}{\partial y} &= \frac{(\alpha_{NW} + 2\alpha_N + \alpha_{NE}) - (\alpha_{SW} + 2\alpha_S + \alpha_{SE})}{8\Delta y} \end{aligned} \quad (2.21)$$

as in Figure 2.2.

## 2.4 Multiphase boundary conditions

In the multiphase problem, boundary conditions become more complicated. The case of a wall boundary condition for a mixed cell has been treated by Braeunig (2007). The flux term for the wall condition is given by:

$$\phi_{wall} = (0, p_{wall}\mathbf{n}, 0) = \frac{\rho_1\tilde{c}_1\mathbf{F}_2 + \rho_2\tilde{c}_2\mathbf{F}_1}{\rho_1\tilde{c}_1 + \rho_2\tilde{c}_2}, \quad (2.22)$$

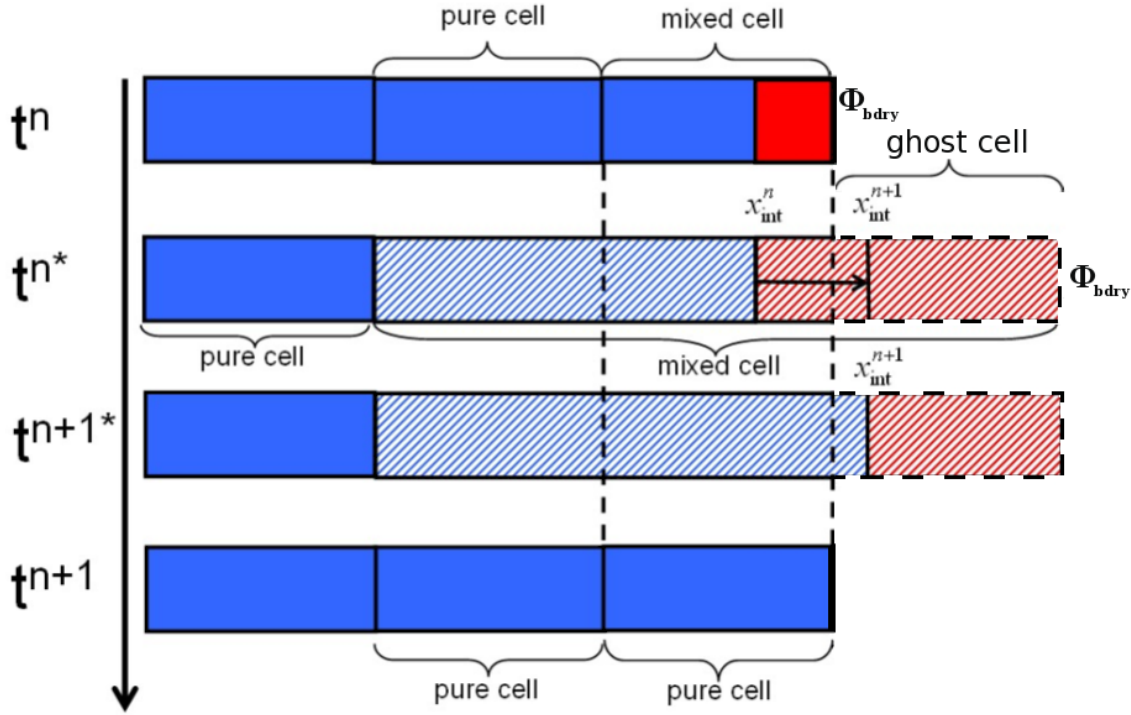


Figure 2.3: Ghost cells

where the subscripts correspond to the two different fluids with conservative variables  $\mathbf{v}_1$  and  $\mathbf{v}_2$ ;  $\tilde{c}_i = \min(c_i, \frac{Vol_i^n}{dtA})$ ; and the  $\mathbf{F}_i$  terms are calculated as the wall boundary flux terms for the single-phase case as given in section 1.5.2.

To handle fluid boundary conditions for mixed cells, I introduce the concept of *ghost cells*. This is a simple numerical technique which allows us to combine the condensate method with the boundary fluxes for single-phase flow presented in section 1.5.1. Given a mixed cell at the boundary with fluid boundary conditions, we create a temporary cell outside the domain to extend the condensate (see Figure 2.4). Using the boundary flux  $\phi_{bdry}$  we calculate the evolution of the condensate as in section 2.3; we then project back onto the Eulerian mesh, discarding the portion which lies outside the boundary. In this way we can handle situations where the interface moves outside the domain, or even cases where a new fluid interface enters the domain.

## Chapter 3

# Numerical results

### 3.1 Test case: faucet flow

In this chapter I present numerical results for the problem of 2D faucet flow. For this problem we have a slightly compressible inviscid liquid falling under gravity in the presence of a compressible gas of much lower density. The liquid falls with initial velocity  $U$  from a pipe of width  $2W$  at a height  $L$  above a horizontal surface. Due to the symmetrical nature of this problem, we consider only the 'right' half of the flow. Thus we have wall conditions on both the left and lower boundaries, and a fluid entry condition on the upper boundary extending  $W$  units from the left wall. The remaining portion of the boundary is assigned Neumann-like boundary conditions, where the external pressure is specified and the density and velocity direction are taken to be constant for the outward flow.

The computational domain begins initially with air, and water enters the domain at a given fixed mass flux. We expect the flow to stabilize as  $t \rightarrow \infty$ . The stabilized flows are then compared with the corresponding stable incompressible flows given by *Christodoulides & Dias*, [5]. We use a scheme that is second-order in space and in time, but only a first-order method at the interface (although a higher-order interface scheme has been developed by *Braeunig*).

Below are the evolutions of several test cases, each with different values of  $H$  and the Froude and Mach numbers. In all cases,  $W = 1$ .

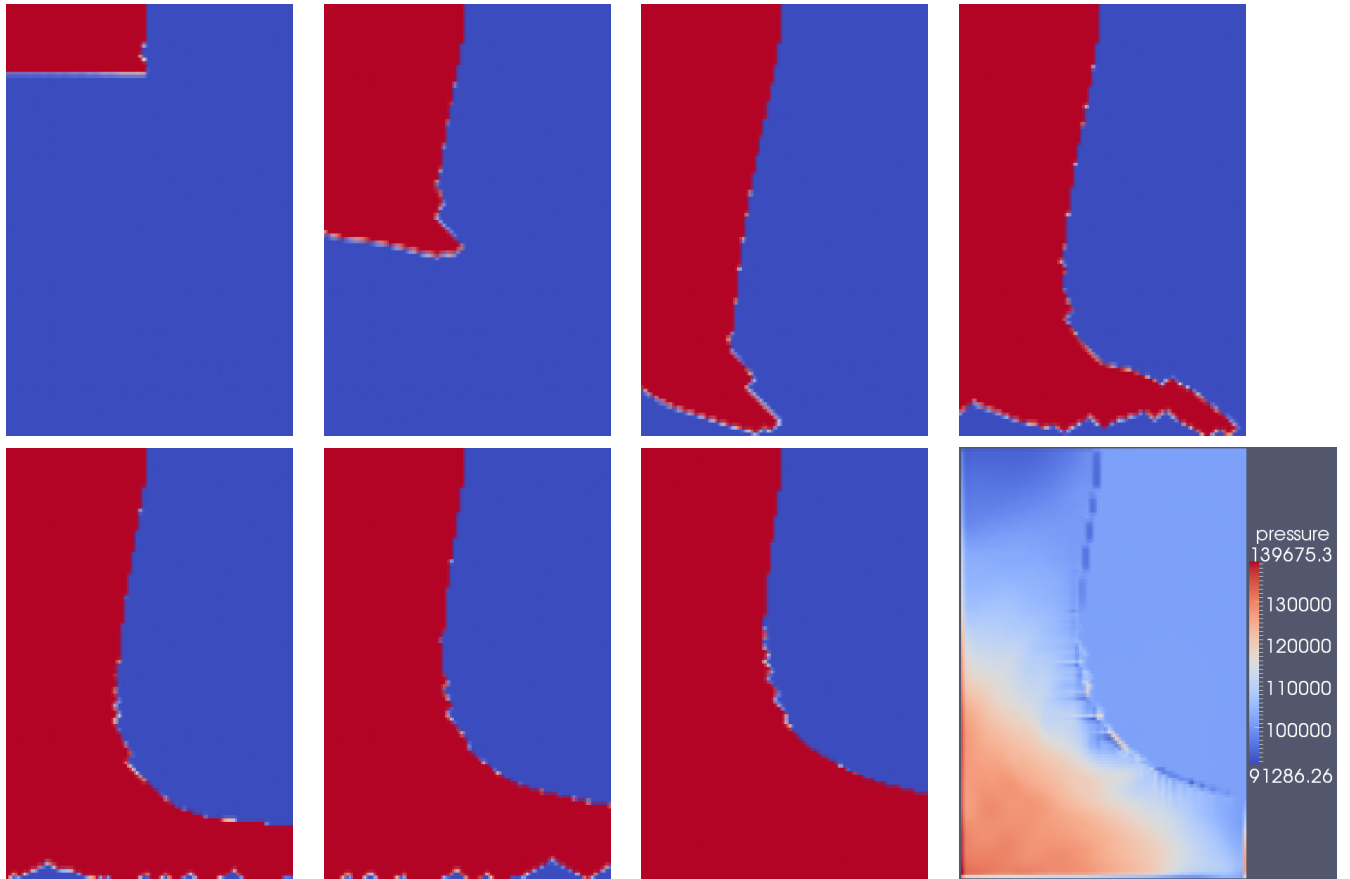


Figure 3.1:  $H = 3.0$ ,  $Fr = 1.5$ ,  $Ma = 0.01175$

The pressure is displayed as the last image of each grouping.

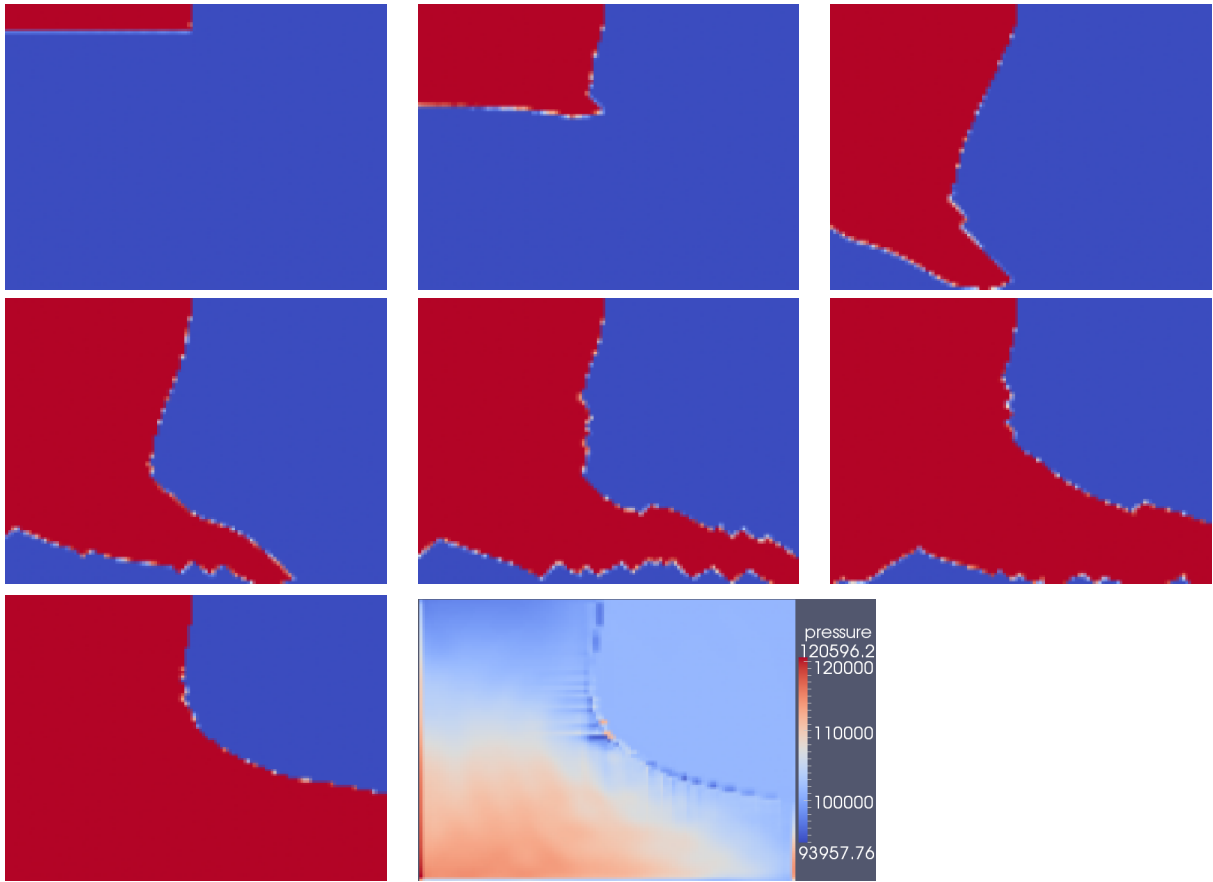


Figure 3.2:  $H = 1.5, Fr = 0.7, Ma = 0.0054775$

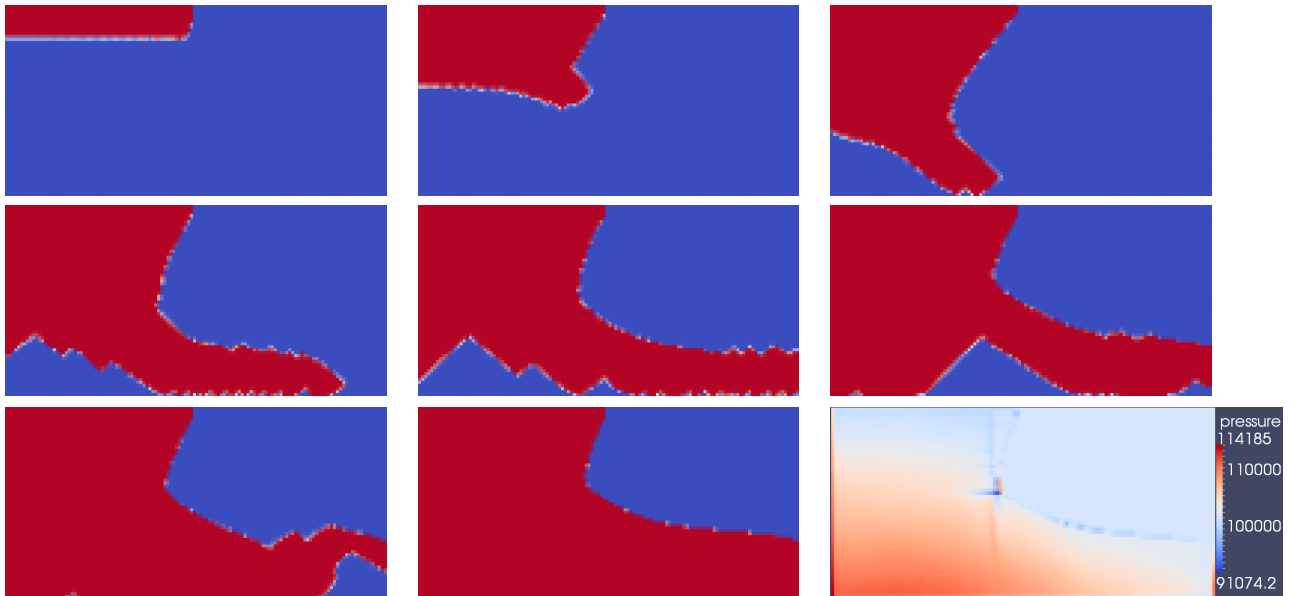


Figure 3.3:  $H = 1.01, Fr = 0.35, Ma = 0.00274$

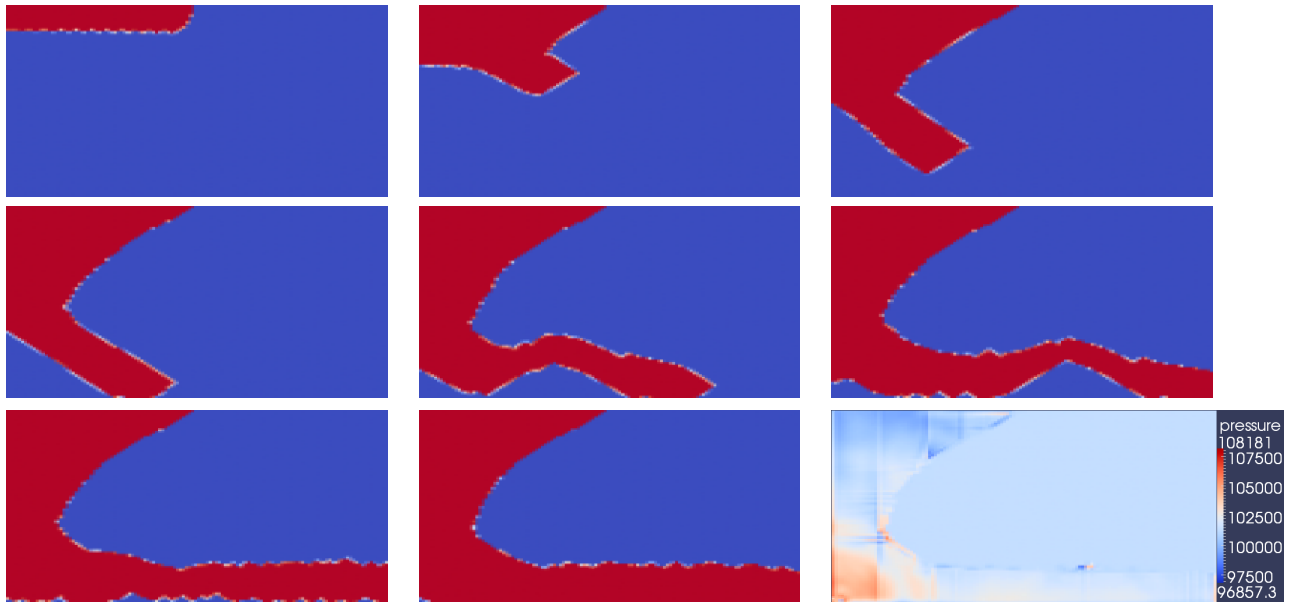


Figure 3.4:  $H = 0.5, Fr = 0.1, Ma = 0.0007285$



Figure 3.5:  $H = 0.2, Fr = 1.5, Ma = 0.1175$

### 3.2 Comparison with incompressible case

The flows presented above correspond to similar incompressible stable flows solved by *Christodoulides & Dias*, [5]. In their formulation, an ideal fluid flows downward through a pipe of width  $W$  with velocity  $U$ , and emerges at a height  $H$  above a horizontal plate. The authors use Bernoulli's equation and a conformal mapping to determine the shape of the free surface for various velocities  $U$ . Their results are compared below with the corresponding compressible results.

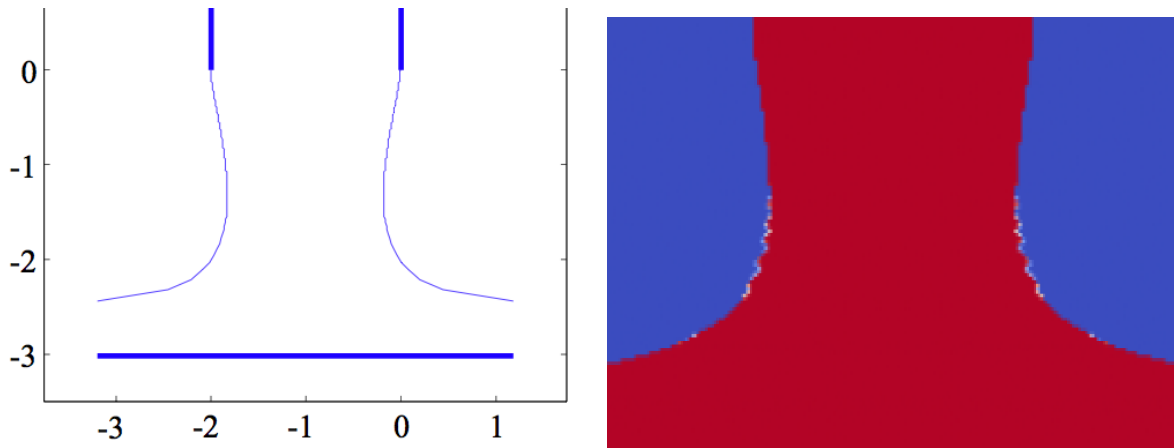


Figure 3.6:  $H = 3.0, Fr = 1.5$

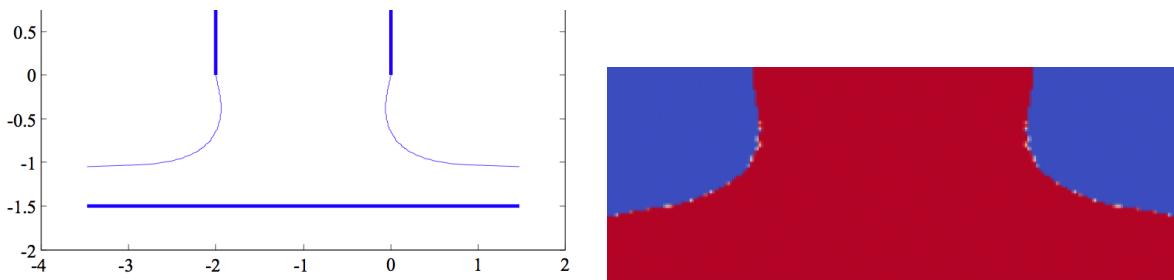


Figure 3.7:  $H = 1.5, Fr = 0.7$

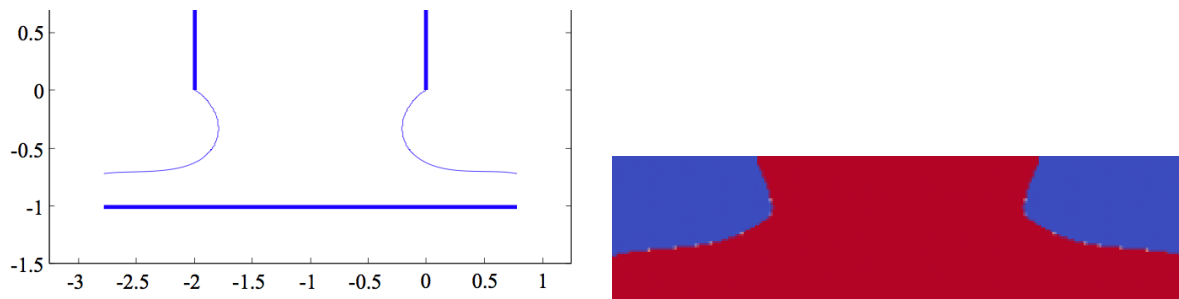


Figure 3.8:  $H = 1.01, Fr = 0.35$

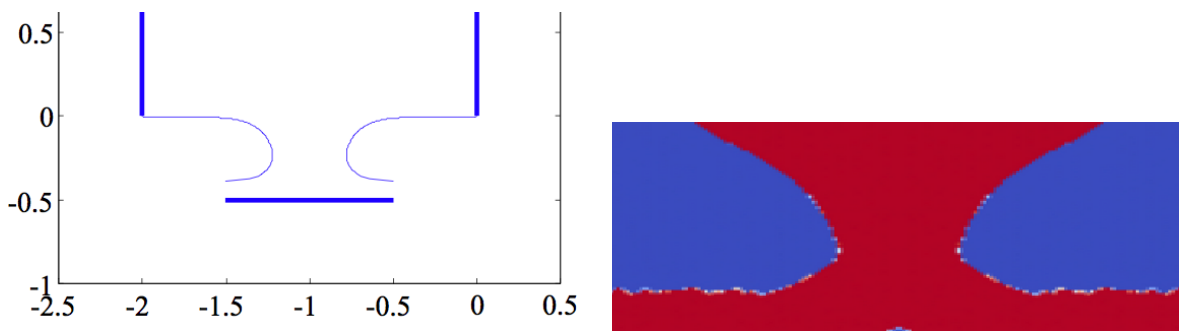


Figure 3.9:  $H = 0.5, Fr = 0.1$

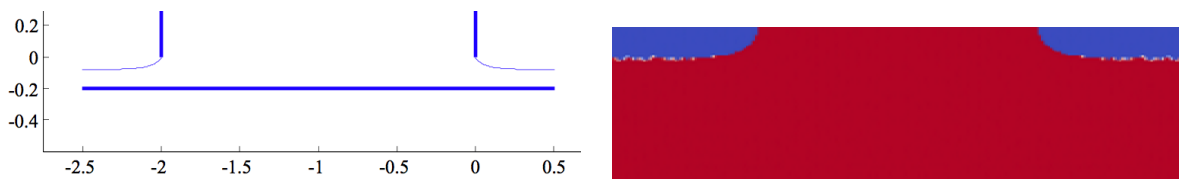


Figure 3.10:  $H = 0.2, Fr = 1.5$



# Bibliography

- [1] J.-M. Ghidaglia, A. Kumbaro, G. Le Coq. Une méthode volumes finis à flux caractéristique pour la résolution numérique des systèmes hyperboliques de lois de conservation. *C.R. Acad. Sc. Paris*, Vol. 322, I, p. 981-988, (1996).
- [2] J.-M. Ghidaglia, F. Pascal. On Boundary Conditions for Multidimensional Hyperbolic Systems of Conservation Laws in the Finite Volume Framework. *CMLA, ENS-Cachan*, (2003).
- [3] B. Youngs. Time-dependent multi-material flow with large fluid distortion. *Numerical Methods for Fluid Dynamics*, p. 273-285, (1982).
- [4] J.-P. Braeunig. Sur la simulation découlements multi-matériaux par une méthode eulérienne directe avec capture d'interfaces en dimensions 1, 2 et 3. *ENS-Cachan*, (2007).
- [5] P. Christodoulides, F. Dias. Impact of a falling jet. *Submitted to publication*.